Int. J. Solids Structures, 1975, Vol. 11, pp. 985–997. Pergamon Press. Printed in Gt. Britain.

THE NON-LINEAR, DYNAMIC RESPONSE OF AN IMPULSIVELY LOADED CIRCULAR PLATE WITH A CENTRAL HOLE

JOSEPH GOLDBERG†
Sr. NSSS Engineer Combustion Engineering, Windsor, CT 06095, U.S.A.

and

HERBERT A. KOENIG‡
Department of Mechanical Engineering, University of Connecticut, Storrs, CT 06268, U.S.A.

(*Received* 29 *September* 1974; *revised* 20 *December* 1974)

Abstract—A numerical method, called Direct Analysis, is described and applied to solve the problem of a plate undergoing a large impulsive load. For generality, an expanded, non-linear form of the equations of motion is used and shear correction and rotatory inertia are considered. The wave speeds are calculated from the non-linear equations and appropriate boundary conditions are applied so that reflected waves are included. The results for two types of step loading pulses are presented and compared with previously presented solutions. The response of the plate is discussed and conclusions as to the effects of the non-linearities are given.

NOMENCLATURE

- A Extensional rigidity $[Eh/(1-\nu^2)]$; lbs/in.
- C_1 Dilatation wave speed; in/sec.
- C_2 Distortion wave speed; in/sec
- C_3 Membrane wave speed; in/sec.
- D Flexural rigidity $[Eh^3/12(1-\nu^2)]$; lb/in.
- E Young's modulus; lbs/in^2.
- e_u^j§ Radial elongation of the jth cell; in/in.
- e_w^j Transverse elongation of the jth cell; in/in.
- e_ϕ^j Angular elongation of the jth cell; rad/in.
- g Gravitational acceleration; in/sec^2.
- G Modulus of rigidity $[E/2(1+\nu)]$; lb/in^2.
- h Plate thickness; in.
- j Superscript referring to quantities of the jth cell.
- j_m Number of cells in plate.
- K_2 Shear correction factor.
- K_m Number of propagation intervals.
- M_r Radial bending moment per unit length; lb-in/in.
- M_θ Tangential bending moment per unit length; lb-in/in.
- N_r Radial membrane force per unit length; lb/in.
- N_θ Tangential membrane force per unit length; lb/in.
- Q_r Radial shear force per unit length; lb/in.
- q Surface force per unit area; lb/in^2.
- r Radial distance; in.
- r_0 Inner radius of the plate; in.
- r_L Outer radius of the plate; in.
- t Time; sec.
- u Radial displacement of plate mid-plane; in.
- $\mathbf{u}$ Radial velocity of plate mid-plane; in/sec.
- w Transverse displacement of plate mid-plane; in.
- $\mathbf{w}$ Transverse velocity of plate mid-plane; in/sec.
- Y_i Generalized displacement field
- $\dot{Y}_i$ Generalized velocity field
- z Transverse distance; in.
- γ Rotation due to shear of plate cross-section; rad.
- ϵ_i Generalized strain field.
- θ Tangential distance; rad.
- ν Poisson's ratio.
- ρ Density of plate; lb/in^3.

†Sr. NSSS Engineer and formerly Graduate Assistant, Department of Mechanical Engineering, University of Connecticut, Storrs, CT 06268, U.S.A.

‡Professor.

§In this work, subscripts are identifying symbols and superscripts are indices in the Direct Analysis Procedure.

τ Material damping constant: sec.
ϕ Rotation due to bending of plate cross-section: rad.
$\dot{\phi}$ Angular velocity of plate; rad/sec.
ψ Total rotation of plate cross-section: rad.

1. INTRODUCTION

A common problem encountered in seismic or accident analysis of nuclear reactor components is the determination of the response of plate-like structures to impact loads. Though the geometries of these plates are rarely regular, the analysis of a simplified annular plate is often used as an approximation for design purposes and it is to this problem that this paper addresses itself.

A numerical method is presented herein to determine the dynamic response of an annular plate with a central hole undergoing an impulsive load. The method, called Direct Analysis, is a numerical technique based on the direct application of the physical laws in finite form. The plate theory used (although the method is applicable to any plate approximation) is non-linear in that second-order terms are retained in the equations of motion as well as in the equations developed to determine the speed of the discontinuities generated by the impact load. Shear correction and rotatory inertia have also been included.

The dynamic solution of plate problems has long been a topic of investigation. Uflyand[1] and Mindlin[2] in separate attempts to generalize the static theory developed a set of equations for the linearized problem, which included shear and rotatory inertia effects. Miklowitz[3] and Lubkin[4], in calculating the stresses in a circular plate due to a suddenly applied transverse load solved these equations by means of integral transforms. Jahsman[5] successfully applied the method of characteristics to the Uflyand-Mindlin equations of motion and his results were improved and generalized by Chou and Koenig[6]. However, finite boundary conditions were not applied in any of these works due to the complexities of including the reflected waves. Recently, a new approach to the solution of dynamic problems was presented by Davids and Koenig[7]. They employed a numerical technique, Direct Analysis, to solve the linear problem of a circular plate with a central hole. The Direct Analysis method includes the interaction of the reflected waves.

In this work, we extend the use of Direct Analysis to solve the non-linear, dynamic plate problem with a central hole. The effects of load magnitude are examined and comparisons between the linear and non-linear stress predictions are presented. The Direct Analysis method is described and all necessary equations are derived.

2. STATEMENT OF PROBLEM

It is known that a plate responds to a rapidly applied load by radiating discontinuities in its physical quantities, i.e. velocities and stresses, that propagate together in groups as waves. We consider in this work, loads that are significantly greater than unity resulting in the propagation of three distinct waves. Presupposing these waves and making a basic set of assumptions, the dynamic response of the plate may be solved for through the use of Direct Analysis.

The assumptions made are: (1) The material is homogeneous, isotropic, and elastic. (2) The plate is thin. (3) The strains are small in comparison with unity. (4) The squares and products of the out-of-plane rotations are of the same order of magnitude as the thickness (Von Karman hypothesis). (5) The deformation is due to both flexural motion and shear deflection of the cross-section.

To obtain the physical laws, the plate is divided, radially and tangentially, into discrete cells. In this work, all cells were selected to be of the same radial length, dr. The selection of the cell pattern (mesh) is, however, arbitrary. The equations of motion are found by applying the Impulse–Momentum laws directly to a typical cell, j, in the deformed state as shown in Fig. 1. The resulting equations,† including the approximations which retain second-order non-linearities are[8]:

†The differential form of these equations, as derived from an elemental volume, are presented in Appendix A.

$$d(u^j) = \frac{\left[N_r^{j+1}r^{j+1}\left(1-\frac{(\phi^{j+1})^2}{2}\right)\right]dt+[Q_r^{j+1}r^{j+1}\phi^{j+1}]dt-\left[N_\theta^j\,dr\left(1-\frac{(\phi^j)^2}{2}\right)\right]dt-\left[N_r^jr^j\left(1-\frac{(\phi^j)^2}{2}\right)\right]dt-[Q_r^jr^j\phi^j]dt}{\frac{\rho}{g}h\left(r^j\,dr+\frac{dr^2}{2}\right)} \tag{1}$$

$$d(w^j) = \frac{-[N^{j+1}r^{j+1}\phi^{j+1}]dt+\left[Q_r^{j+1}r^{j+1}\left(1-\frac{(\phi^{j+1})^2}{2}\right)\right]dt+[N_r^jr^j\phi^j]dt-\left[Q_r^jr^j\left(1-\frac{(\phi^j)^2}{2}\right)\right]dt+[N_\theta^j\,dr\phi^j]dt+\left[q\left(r^j\,dr+\frac{dr^2}{2}\right)\right]dt}{\frac{\rho}{g}h\left(r^j\,dr+\frac{dr^2}{2}\right)} \tag{2}$$

$$d(\phi^j) = \left[\begin{array}{c} [M_r^{j+1}r^{j+1}]dt-[M_r^jr^j]dt-\left[Q_r^{j+1}r^{j+1}\left(1-\frac{(\phi^{j+1})^2}{2}\right)\left(\frac{dr}{2}+\frac{u^{j+1}-u^j}{2}\right)\right]dt \\ -\left[Q^{j+1}r^{j+1}\phi^{j+1}\left(\frac{w^{j+1}-w^j}{2}\right)\right]dt-\left[N_r^{j+1}r^{j+1}\left(1-\frac{\phi^{j+1})^2}{2}\right)\left(\frac{w^{j+1}-w^j}{2}\right)\right]dt \\ +\left[N_r^{j+1}r^{j+1}\phi^{j+1}\left(\frac{dr}{2}+\frac{u^{j+1}-u^j}{2}\right)\right]dt-\left[Q_r^jr^j(1-\frac{(\phi^j)}{2})\left(\frac{dr}{2}+\frac{u^{j+1}-u^j}{2}\right)\right]dt \\ -[Q_r^jr^j\phi^j\left(\frac{w^{j+1}-w^j}{2}\right)]dt-\left[N_r^jr^j(1-\frac{(\phi^j)^2}{2})\left(\frac{w^{j+1}-w^j}{2}\right)\right]dt \\ +\left[N^jr^j\phi^j\left(\frac{dr}{2}+\frac{u^{j+1}-u^j}{2}\right)\right]dt-\left[M_\theta^j\,dr\right]dt \\ -\left[q\left(r^j\,dr+\frac{dr^2}{r}\right)\frac{dr}{6}\right]dt \\ \hline \frac{\rho h^3}{12\,g}\left(r^j\,dr+\frac{dr^2}{2}\right) \end{array}\right]. \tag{3}$$

Assuming a linear constitutive law, the relations between the stress resultants (called the forces and moments) and the strain components may be found by integrating Hook's law through the thickness of the plate.

$$M_r^{j+1} = \frac{Eh^3}{12(1-\nu^2)}\left[e_\phi^{\,j}+\nu\frac{\phi^j}{r^j}\right] \tag{4}$$

$$M_\theta^j = \frac{Eh^3}{12(1-\nu^2)}\left[\frac{\phi^j}{r^j}+\nu e_\phi^{\,j}\right] \tag{5}$$

$$N_r^{j+1} = \frac{Eh}{1-\nu^2}\left[e_u^{\,j}+\frac{1}{2}(e_w^{\,j})^2+\nu\frac{u^j}{r^j}\right] \tag{6}$$

$$N^j = \frac{Eh}{1-\nu^2}\left[\frac{u^j}{r^j}+\nu e_u^{\,j}+\frac{\nu}{2}(e_w^{\,j})^2\right] \tag{7}$$

where:

$$e_u^{\,j} = \frac{u^{j+1}-u^j}{dr} \tag{8}$$

$$e_w^{\,j} = \frac{w^{j+1}-w^j}{dr} \tag{9}$$

$$e_\phi^{\,j} = \frac{\phi^{j+1}-\phi^j}{dr}. \tag{10}$$

We note that, as in linear theory $\sigma_{rz} = 0$; consequently, $Q_r = 0$. However, following the lead of previous work[7, 9], we apply assumption 5 in an attempt to correct for the neglected shear.

Postulating that the total rotation of a typical element is the result of the two assumed contributions to the deformation, viz:

$$\psi = \phi + \gamma. \tag{11}$$

We propose that the shear force be proportional to the shear angle, γ.

$$Q_r^{j+1} = (K_2)^2 Gh(\phi^{j+1} + e_w^j) \tag{12}$$

where K_2 is a constant given by[3]:

$$(K_2)^2 = 0{\cdot}76 + 0{\cdot}3\nu. \tag{13}$$

The speed of propagation may be calculated by applying the method of characteristics to the nonlinear equations of motion[8] and solving for the physical characteristics. It was found that discontinuities in M_r, M_θ, ϕ, and their derivatives propagate together at the dilatational wave speed:

$$C_1^j = \left[\frac{E}{\frac{\rho}{g}(1-\nu^2)}\right]^{1/2}. \tag{14}$$

Similarly, discontinuities in Q_r, $\mathbf{w}$, and their derivatives propagate at the distortional (shear) wave speed:

$$C_2^j = \left[\frac{(AZ^j + \beta^j) - [(AZ^j + \beta^j)^2 - 4(AZ^j\beta^j + A\phi^j\alpha^j)]^{1/2}}{2\frac{\rho}{g}h}\right]^{1/2}. \tag{15}$$

Finally, the membrane (in-plane) wave speed, at which discontinuities in N_r, N_θ, $\mathbf{u}$, and their derivatives propagate, is:

$$C_3^j = \left[\frac{(AZ^j + \beta^j) + [(AZ^j + \beta^j)^2 - 4(AZ^j\beta^j + A\phi^j\alpha^j)]^{1/2}}{2\frac{\rho}{g}h}\right]^{1/2} \tag{16}$$

where:

$$Z^j = 1 - \frac{(\phi^j)^2}{2} \tag{17}$$

$$A = \frac{Eh}{(1-\nu^2)} \tag{18}$$

$$\alpha^j = Ae_w^j Z^j + (K_2)^2 Gh\phi^j \tag{19}$$

$$\beta^j = -Ae_w^j\phi^j + (K_2)^2 GhZ^j. \tag{20}$$

Any loading input to the plate results in all three waves being generated as is seen from the coupling of equations (1–7) and (12). We also note that the magnitudes of the distortional and membrane wave speeds change with the fluctuating state of the plate.

A static solution may be obtained by expressing the internal material damping of the plate. A damping rule may be arbitrarily selected to reduce the response of the body at each calculational step of the method. As time progresses, the velocity of the plate is continuously reduced until the incremental motion becomes negligible; i.e. the static state is reached. Assuming an exponential damping rule, viz:

$$\mathbf{Y}_i^j = \mathbf{Y}_{0_i}^j e^{-t/\tau}$$

where τ is an arbitrary time constant, and Y_1, Y_2, Y_3 are ϕ, w, and u, respectively. Y_0 is the initial value of the velocity at the current instant of time. Since, in the method, the incremental time changes through real time are not constant (they change with wave speed), the ratio t/τ may be set as a constant. This allows for constant damping throughout the problem. If we select this ratio to be small, the motion is almost totally unrestrained since the damping effect would be negligible. The undamped case results. If t/τ is specified large, we allow almost no motion to occur.

The boundary conditions for the plate must be formulated with the special conditions of the shear-corrected theory in mind. For the case of a clamped outer edge, the boundary conditions are:

$$\phi^{i_m+1} = 0 \tag{21}$$

$$w^{i_m+1} = 0 \tag{22}$$

$$u^{i_m+1} = 0. \tag{23}$$

Although the rotation, ϕ, at the outer edge is zero, we see that the slope need not be, since the cross-section may undergo a shear rotation at the clamped end.

Equations (1–23) comprise the full set of physical laws required to describe the non-linear, dynamic plate problem. Direct Analysis is applied to these equations to effect a solution.

3. DISCUSSION OF DIRECT ANALYSIS

Direct analysis is a numerical technique that is easily applied through the use of a digital computer. In this method, the physical laws are directly satisfied within discrete portions (cells) of the plate in a sequential manner. The sequence is determined by the motion of the three waves which propagate. Each wave requires a different finite time interval, $dt = dx/C$ (the characteristic statement), to travel through a cell. Whenever the time interval required for a wave to travel through a cell has elapsed, the wave front is propagated by the calculation of an incremental change in the associated physical quantities by means of the appropriate physical laws. The state of the plate is "updated" by cumulating the change to its existing condition.

The continued wave sequence, with continued propagations, maintains the plate at the correct dynamic state. The values of the incremented variables must, however, be changed in all of the physical laws to insure numerical accuracy. Due to the coupling of the physical laws, certain portions of the equations require intermediate adjustments. To accomplish this, each portion of the physical laws is treated as an individual function which is updated separately. Also, as previously mentioned, the speed of propagation must continuously be adjusted to insure correct propagation intervals.

The Direct Analysis method is presented in [8]; we now present a summary of the procedure. We divide the computer code into three main parts. (A) The main body of the procedure that coordinates the calculations. (B) The computation routines for each wave. (C) The routine to calculate the wave speeds. Using equations (1–23), the procedure would be as follows:

Part 1: *Main body of the procedure*: *BEGIN*

(1) Specify material properties; plate geometry and solution characteristics.

$$E, \rho, \nu, \tau_i, r_0, r_L, h, dr, \text{and } K_m$$

(2) Specify initial state of plate, initial conditions, and initial loading. All input conditions are specified at the appropriate points of the mesh.

(3) Calculate all wave speeds: Part 3.

(4) Calculate dt (characteristic statement) for each wave in each cell; determine the minimum realtime, dt, required for any wave in any cell to propagate and propagate that wave; Time is incremented: $t = t + dt$.

(5) Calculate and cumulate new incremental variables corresponding to the existing dynamic conditions: Part 2.

(6) Record new state of the plate.

(7) Check to see if the required time has passed.

$$\text{If } t \geq K_m \, dt \begin{cases} \text{no: go to Step (3)} \\ \text{yes: STOP} \end{cases}$$

Part 2: *Wave propagation routines*

(1) Begin Loop 1: Do steps for each cell, j that contains a wave, i, that has propagated.

(a) Calculate and cumulate all Impulse Functions (all portions of the Equations of Motion that are related to wave i).

(b) Apply the first half of damping; $\mathbf{Y}_i^j = \mathbf{Y}_i^j = \mathbf{Y}_i^j(dt/2\tau_i)$.

(c) Calculate the incremental change in $\mathbf{Y}_i^j$; *If* $i = 1$, 2, or 3, use equations (3), (2) or (1), respectively. Cumulate the new increment; $\mathbf{Y}_i^j = \mathbf{Y}_i^j + d\mathbf{Y}_i^j$.

(d) Specify the boundary condition;

$$\mathbf{Y}_i^{j_m+1} = 0$$

(e) Apply the second half of damping;

$$\mathbf{Y}_i^j = \mathbf{Y}_i^j - \mathbf{Y}_i^j \, (dt/2\tau_i)$$

(f) Zero those Impulse Functions used to calculate the new increment.

(2) End Loop 1; Begin Loop 2: Do steps for each cell, j, that contains a wave i, that has propagated.

(a) Calculate the elongation

$$e_i^j = \frac{(\mathbf{Y}_i^{j+1} - \mathbf{Y}_i^j)dt}{dr}$$

(b) Calculate the stress increments from the constitutive relations and cumulate the incremental change.

$$\text{If } i = \begin{matrix} 1 \\ 2; \\ 3 \end{matrix} \text{ Then apply equations } \begin{matrix} \text{4, 5 and the first portion of 12} \\ \text{6, 7 and the second portion of 12} \\ \text{6 and 7} \end{matrix}$$

(c) Calculate the incremental change in the displacement

$$Y_i^j = Y_i^j + \dot{Y}_i^j \, (dt)$$

(3) End Loop 2.

Part 3: *Wave speed routine*

(1) Loop 1: ($j = 1, 2, \ldots, j_m$)

(a) Calculate dilatational wave speed from Equation 14.

(b) Calculate distortional wave speed from Equation 15.

(c) Calculate membrane wave speed from Equation 16.

(2) End Loop 1.

The procedure is brought to an end when a preselected amount of propagations has been completed. We note that in Part 2, Sections (b) and (e), the damping is applied in halves. It was found that this resulted in increased numerical stability in the overall procedure.

Iteration within each cell is unnecessary, as continuous updating within each cell maintains the cell at the correct, current dynamic state. However, since calculations are performed in a cumulative manner, round-off error (inherent in all digital computer calculations) may become significant after prolonged application of the code. The size of the round-off error, and the accuracy of the method itself, is dependent on a number of parameters such as cell size and sequence of procedural steps.

4. DISCUSSION OF RESULTS

The Direct Analysis is applied to solve a number of sample problems in this section. Two problem that do not include damping are considered. These problems were selected for their

computational efficiency and are only samples. Any geometrical configuration may be input. The results show the fluctuations of the stress field for the first 6 microseconds after the load is applied.

The material properties for the problems are:

$$E = 28 \times 10^6 \text{ psi}, \nu = 0{\cdot}3, \rho = 0{\cdot}286 \text{ lb/in}^3 \text{ and } dt/\tau_{1,2} \text{ and } 3 = 0$$

The plate specifications for the first problem are:

$$r_0 = 0{\cdot}025 \text{ in.}, r_L = 0{\cdot}30 \text{ in., and } h = 0{\cdot}125 \text{ in.} \tag{25}$$

The loading for this problem is applied at the inner edge of the plate and is as follows:

$$\begin{aligned} &(1)\ (a)\ Q_r(r_0, t) = 0{\cdot}001 \text{ lbs/in.} \\ &\quad\ (b)\ Q_r(r_0, t) = 10 \text{ lbs/in.} \end{aligned}$$

In the second problem considered, we specify the following plate dimensions.

$$r_0 = 0{\cdot}25 \text{ in.}, r_L = 0{\cdot}85 \text{ in., and } h = 0{\cdot}125 \text{ in.} \tag{26}$$

The loading is also supplied at the inner edge and is

$$\begin{aligned} &(2)\ (a)\ M_r(r_0, t) = 0{\cdot}001 \text{ in.-lbs/in.} \\ &\quad\ (b)\ M_r(r_0, t) = 10 \text{ in.-lbs/in.} \end{aligned}$$

For both these problems, there are no applied surface loading i.e. $q = 0$, and the outer edge is clamped.

Parameters such as boundary conditions, plate dimensions, and damping values are inputs to the computer code and may be easily changed from problem to problem. Also, any loading condition may be represented discretely as a series of appropriately adjusted step functions.

(1) For the first problem with the smaller load applied, the resulting initial wave speeds are $C_1 = C_3 = 0{\cdot}204 \times 10^6$ in./sec., and $C_2 = 0{\cdot}111 \times 10^6$ in./sec., which are equivalent to the linear case (the membrane wave does not appear in the linearized problem). At these speeds, it takes approximately 1·35 microseconds for the dilatational and membrane waves to traverse the plate and 2·48 microseconds for the distortional wave. Selecting $r = 0{\cdot}125$ in. as the point of inspection, Figs. 2, 3 and 4 show the radial moment, tangential moment, transverse shear, radial membrane force and tangential membrane force, respectively. Since the applied load is small in comparison to unity, the problem is linear; that is, the nonlinear terms are negligible in comparison with the other terms. This is demonstrated by comparison of the results with the solution presented by Koenig[11], which is given in Figs. 2 and 3. Due to the linearity of the problem, the wave speeds remain constant for the 6 microseconds. Examining the Figs., we see that the dilatational and membrane waves lead the distortional wave. The delay in the arrival of the distortional wave at the point of inspection results in an initial calculation of a negative transverse shear, due to the coupling of the shear to the dilatational effects. When the distortional wave arrives, a positive transverse shear is calculated as expected. Figures 2 and 3 include the results of Chou and Koenig[6] for the case of an infinite plate with a central hole. In Fig. 2, we see that the results agree quite well for the first 2·0 microseconds. However, we do not present results beyond this time since reflected waves were not considered in their work. We note that the reflected waves cause rapid fluctuation of the stress field and that the forces and moments generally increase with the interaction. Examining Fig. 4, we see that the in-plane forces are considerably smaller than the moments and shear. Figures 5, 6 and 7 present the moments and forces for a similar problem with an increased step shear input, $Q_r(r_0, t) = 10$ lbs/in. The results of this nonlinear problem are compared with the results predicted by the linear problem with the larger load applied. We see that the included nonlinearities significantly reduced the moments and forces in the plate. Forming the ratio between peak shear, linear to nonlinear, we obtain at 5·8 microseconds:

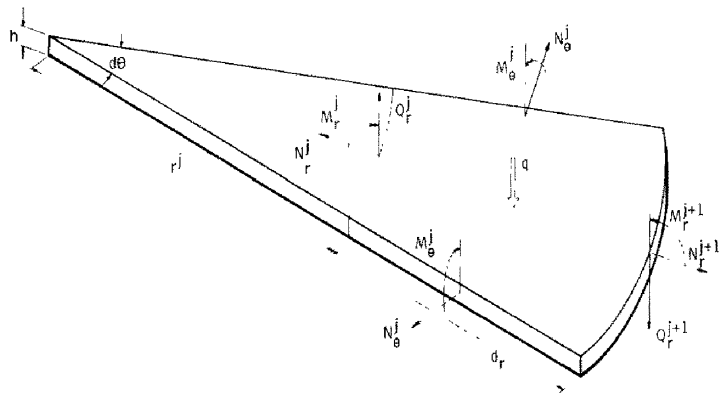

Fig. 1. jth Plate element in deformated state.

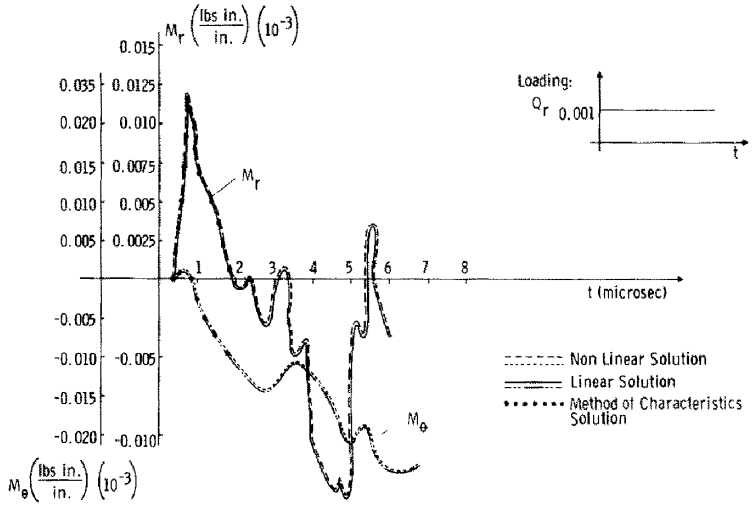

Fig. 2. Radial and tangential moment vs time at $r = 0{\cdot}125$ in.

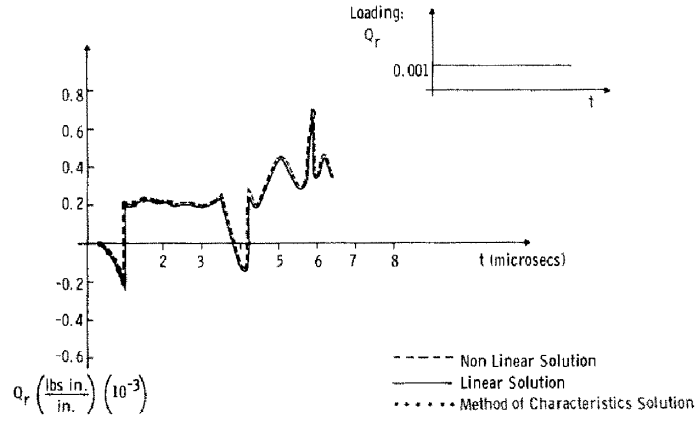

Fig. 3. Radial shear vs time at $r = 0{\cdot}125$ in.

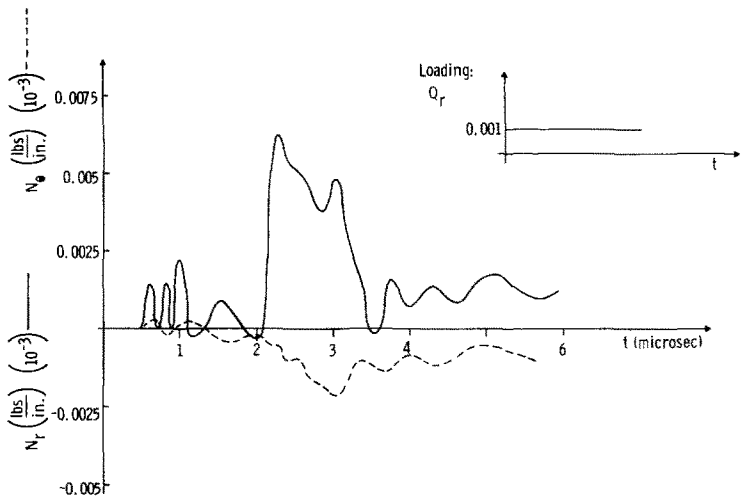

Fig. 4. Radial and tangential membrane force vs time at $r = 0{\cdot}125$ in.

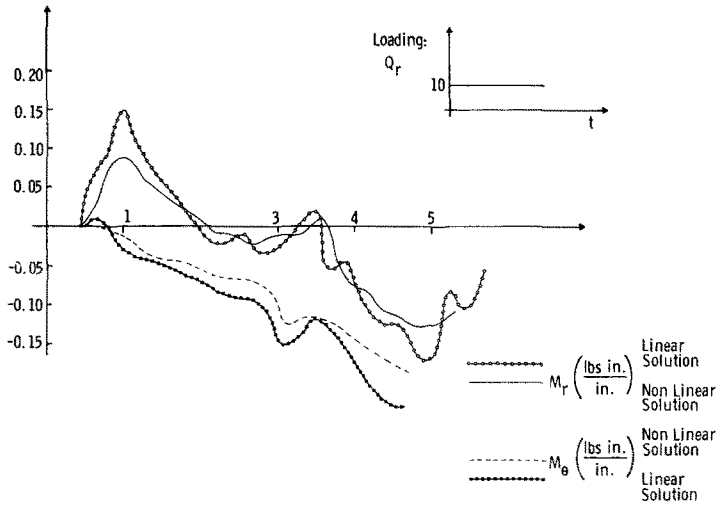

Fig. 5. Radial and tangential moment vs time at $r = 0{\cdot}125$ in.

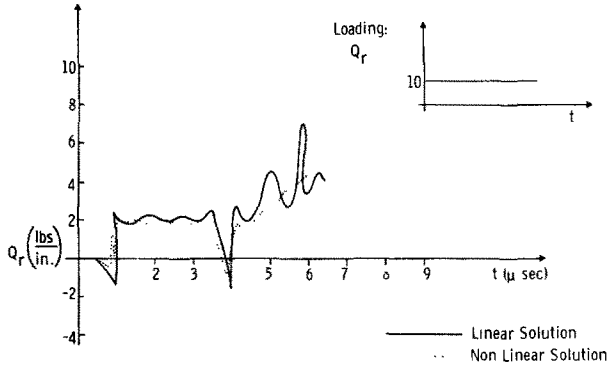

Fig. 6. Radial shear vs time at $r = 0{\cdot}125$ in.

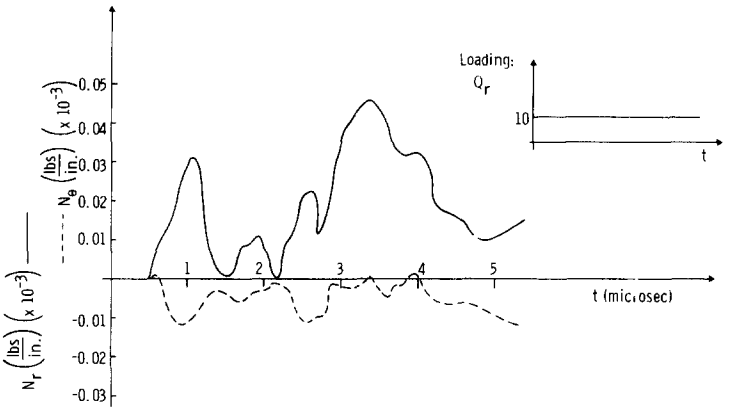

Fig. 7. Radial and tangential membrane force vs time at $r = 0{\cdot}125$ in.

$$\frac{Qr_{\text{linear}}}{Qr_{\text{nonlinear}}} = \frac{7{\cdot}0}{4{\cdot}2} = 1{\cdot}67 \tag{27}$$

The linearized analysis significantly over-estimates the shear. Consequently, the use of the linear theory in applications where larger loading and/or larger deflections take place would result in an over-designed structure. Figure 6 shows the distortional wave arriving earlier in the nonlinear solution than in the linear. This indicates that the distortional wave speed has generally increased, though its value fluctuates from cell to cell. Similarly, it was found that the membrane wave decreased in speed.

(2) The results of the second problem with step moment input of $M_r(r_0, t) = 0{\cdot}001$ in.-lbs/in., are presented in Figs. 8–10 with the point of inspection at $r = 0{\cdot}375$ in. The problem is then repeated with the step moment increased to 10 in.-lbs/in.; the results are given in Figs. 11–13. Again, the results of the smaller load problem agree well with the linear solution and the wave speeds remain essentially constant. We observe that the moments and forces fluctuate greatly with the wave interactions and that the field is significantly increased by these dynamic effects. Once again, the membrane forces remain considerably smaller than the moments and shear. Comparing the linear and nonlinear analyses in Figs. 11–13 for the larger load problem, we see that the nonlinear effects are equivalent to the nonlinear effects in the shear input problem. The stress field is generally reduced by the included nonlinearities and the wave speeds fluctuate greatly. The shear wave speed increases while the membrane wave speed decreases. Any plate structure, designed with the results of the linear problem would over-compensate for the stresses induced by a large radial moment impulsive load.

4. CLOSURE

This article utilized the Direct Analysis method to solve the nonlinear dynamic problem of an impulsively loaded plate. A description of the method was given and the specific physical laws required were derived. Two example problems were worked and the results compared to previously presented solutions. With loads that were large compared to unity, it was found that: (1) The stress distributions did significantly vary from previous results and were generally smaller than previously predicted. (2) The pattern of wave speed changes tended to increase the significance of the shear related quantities and decrease the significance of the membrane related quantities.

The following conclusions were drawn in regards to the method. (1) The Direct Analysis method is an accurate numerical technique for the determination of the dynamic nonlinear response of a circular plate with a central hole that undergoes impulsive type loadings. (2) Changes in input loading and boundary conditions offered no additional complexity. (3) The results agree with previously linear solutions and provide more accurate predictions for problems with larger loads and/or displacements.

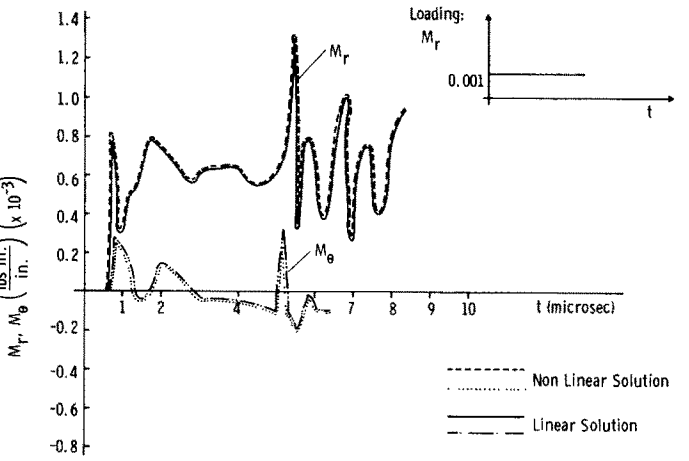

Fig. 8. Radial and tangential moment vs time at $r = 0{\cdot}375$ in.

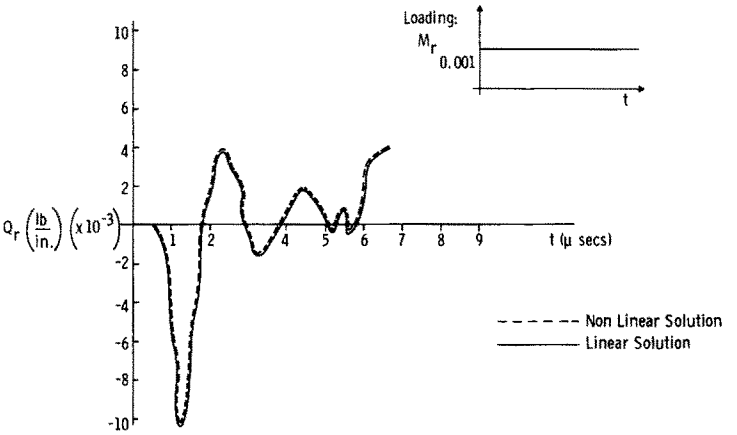

Fig. 9. Radial shear vs time at $4 = 0{\cdot}375$ in.

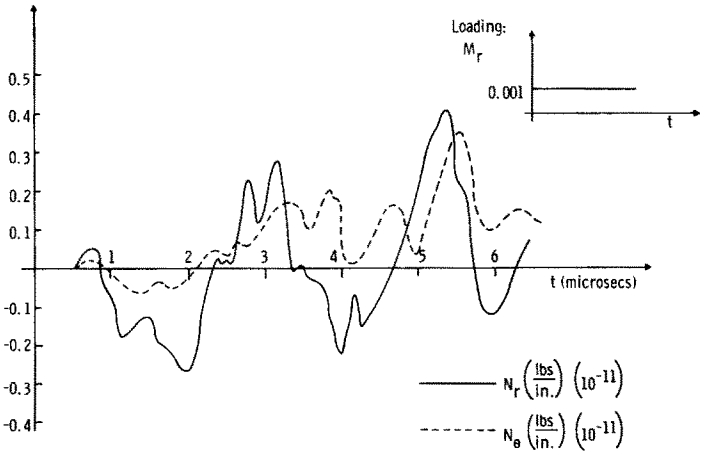

Fig. 10. Radial and tangential membrane force vs time at $r = 0{\cdot}375$ in.

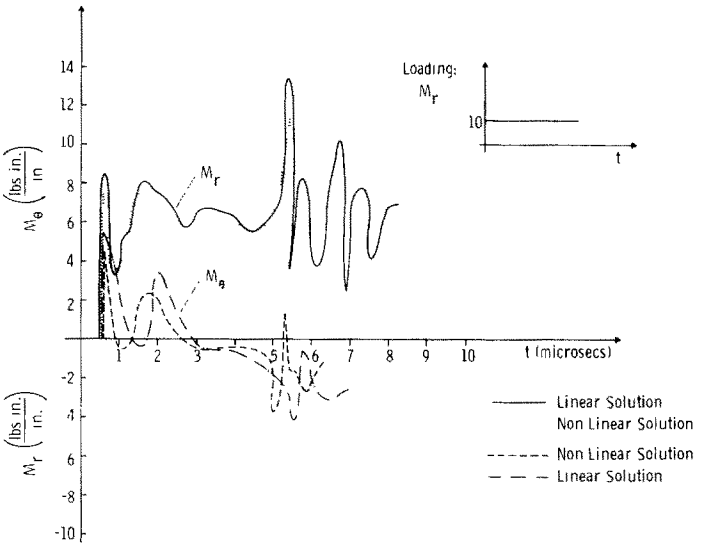

Fig. 11. Radial and tangential moment vs time at $r = 0{\cdot}375$ in.

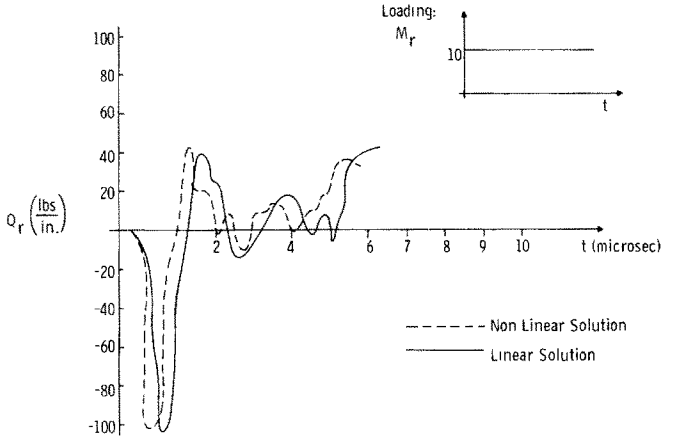

Fig. 12. Radial shear vs time at $r = 0{\cdot}375$ in.

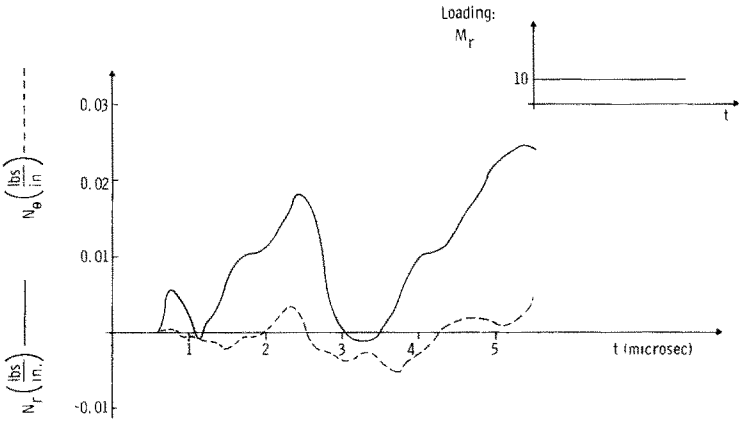

Fig. 13. Radial and tangential membrane force vs time at $r = 0{\cdot}375$ in.

REFERENCES

1. Y. S. Uflyand, The propagation of waves in transverse vibrations of bars and plate. *Prikl. Mat. Mch.* **12**, p. 287 (1948).
2. R. C. Mindlin, Influence of rotatory inertia and shear on flexural motion of isotropic, elastic plates. *J. Appl. Mech.* **18** 31 (1951).
3. J. Miklowitz, Flexural stress waves in an indefinite elastic plate due to a suddenly applied concentrated transverse load. *J. Appl. Mech.*, pp. 681–689 (Dec., 1960).
4. J. L. Lubkin, Propagation of elastic stress waves. ONR Progress Report # 5, Contract # NONR-704(00) (1954).
5. W. E. Jahsman, Propagation of abrupt circular wave fronts in elastic sheets and plates. *Proc. of 3rd Congress on Appl. Mech.* pp. 115–202 (1958).
6. P. C. Chou, and H. A. Koenig, Flexural waves in elastic circular plates by method of characteristics. DRT Report No. 160–6 (Aug., 1965).
7. N. Davids and H. A. Koenig, Dynamical finite element analysis for elastic waves in beams and plates. *Int. J. Solids Struc.* **4**, (1968).
8. J. Goldberg, The dynamic, non-linear response of a circular plate with a central hole by direct analysis. Thesis in Mechanical Engineering, University of Connecticut, Storrs (1975).
9. N. Davids and H. A. Koenig, Direct analysis of flexural travelling waves in beams and plates. Penn. St. Univ., Eng. Bulletin No. 1 (1966).
10. S. Timoshenko and S. Woinowsky-Krieger, *Theory of Plates and Shells*, 2nd Ed. McGraw Hill Book Co. (1959).
11. H. A. Koenig, Multiple stress wave discontinuities in finite beams and plates. Thesis in Engineering Mechanics, Pennsylvania State University (1967).

APPENDIX A

Presuming Fig. 1 to be a representation of an elemental volume, the following differential equations of motion are found (note that these are equations (1–3) in differential form).

$$(N_r + N_{r,r}\,dr)(r+dr)\,d\theta\left(1-\frac{\alpha^2}{2}\right)+(Q_r+Q_{r,r}\,dr)(r+dr)\,d\theta\alpha-2N_\theta\,dr\frac{d\theta}{2}\left(1-\frac{\phi^2}{2}\right)$$

$$-N_r r\,d\theta\left(1-\frac{\phi^2}{2}\right)-Q_r r\,d\theta\phi=\frac{\rho h}{g}\left(r\,dr+\frac{dr^2}{2}\right)d\theta u_{,tt} \tag{A.1}$$

$$-(N_r+N_{r,r}\,dr)(r+dr)\,d\theta\alpha+(Q_r+Q_{rr,r}\,dr)(r+dr)\,d\theta\left(1-\frac{\alpha^2}{2}\right)+N_r r\,d\theta\phi$$

$$-Q_r r\,d\theta\left(1-\frac{\phi^2}{2}\right)+q\left(r\,dr+\frac{dr^2}{2}\right)d\theta+2N_\theta\,dr\frac{d\theta}{2}\phi=\frac{\rho h}{g}\left(r\,dr+\frac{dr^2}{2}\right)d\theta w_{,tt} \tag{A.2}$$

$$-M_r r\,d\theta+(M_r+M_{r,r}\,dr)(r+dr)\,d\theta-Q_r r\,d\theta\left(1-\frac{\phi^2}{2}\right)\left(\frac{dr}{2}+\frac{1}{2}u_{,r}\,dr\right)$$

$$-Q_r r\,d\theta\,\phi\left(\frac{1}{2}w_{,r}\,dr\right)-N_r r\,d\theta\left(1-\frac{\phi^2}{2}\right)\left(\frac{1}{2}w_{,r}\,dr\right)+N_r r\,d\theta\phi\left(\frac{dr}{2}+\frac{1}{2}u_{,r}\,dr\right) \tag{A.3}$$

$$-(Q_r+Q_{r,r}\,dr)(r+dr)\,d\theta\left(\frac{1}{2}w_{,r}\,dr\right)\alpha-(Q_r+Q_{r,r}\,dr)(r+dr)\,d\theta\left(1-\frac{\alpha^2}{2}\right)\left(\frac{dr}{2}+\frac{1}{2}u_{,r}\,dr\right)$$

$$-(N_r+N_{r,r}\,dr)(r+dr)\,d\theta\left(1-\frac{\alpha^2}{2}\right)\left(\frac{1}{2}w_{,r}\,dr\right)+(N_r+N_{r,r}\,dr)(r+dr)\,d\theta\alpha\left(\frac{dr}{2}+\frac{1}{2}u_{,r}\,dr\right)$$

$$-q\left(r\,dr+\frac{dr^2}{2}\right)d\theta\frac{dr}{6}-2M_\theta\,dr\frac{d\theta}{2}=\frac{\rho h^3}{12g}\left(r\,dr+\frac{dr^2}{2}\right)d\theta\phi_{,tt}.$$

Where a comma indicates partial differentiation and

$$\alpha=\phi+\phi_{,r}\,dr \tag{A.4}$$

The geometric approximations in the above equations were:

$$\sin\Omega\approx\Omega \tag{A.5}$$

$$\cos\Omega\approx1-\frac{\Omega^2}{2}. \tag{A.6}$$

Where Ω is a small angle.